Wein AN, Liu S, Zhang Y et al (2013) Tumor therapy with a urokinase plasminogen activator-activated anthrax lethal toxin alone and in combination with paclitaxel. Invest New Drugs 31:206–212. doi:10.1007/s10637-012-9847-1

Wei W, Lu Q, Chaudry GJ et al (2006) The LDL receptor-related protein LRP6 mediates internalization and lethality of anthrax toxin. Cell 124:1141–1154. doi:10.1016/j.cell.2005.12.045, S0092-8674(06)00199-1 [pii]

Wesche J, Elliott JL, Falnes PO et al (1998) Characterization of membrane translocation by anthrax protective antigen. Biochemistry 37:15737–15746

Wigelsworth DJ, Krantz BA, Christensen KA et al (2004) Binding stoichiometry and kinetics of the interaction of a human anthrax toxin receptor, CMG2, with protective antigen. J Biol Chem 279:23349–23356

Williams P, Wallace D (1989) Unit 731: Japan's secret biological warfare in World War II. Free Press, New York

Wimalasena DS, Cramer JC, Janowiak BE et al (2007) Effect of 2-fluorohistidine labeling of the anthrax protective antigen on stability, pore formation, and translocation. Biochemistry 46:14928–14936. doi:10.1021/bi701763z

Wolfe JT, Krantz BA, Rainey GJ et al (2005) Whole-cell voltage clamp measurements of anthrax toxin pore current. J Biol Chem 280:39417–39422

Wright GG, Hedberg MA, Slein JB (1954) Studies on immunity in anthrax. III. Elaboration of protective antigen in a chemically defined, non-protein medium. J Immunol 72:263–269

Wynia-Smith SL, Brown MJ, Chirichella G et al (2012) Electrostatic ratchet in the protective antigen channel promotes anthrax toxin translocation. J Biol Chem 287:43753–43764. doi:10.1074/jbc.M112.419598, M112.419598 [pii]

Young JA, Collier RJ (2007) Anthrax toxin: receptor binding, internalization, pore formation, and translocation. Annu Rev Biochem 76:243–265. doi:10.1146/annurev.biochem.75.103004.142728

Young JJ, Bromberg-White JL, Zylstra C et al (2007) LRP5 and LRP6 are not required for protective antigen-mediated internalization or lethality of anthrax lethal toxin. PLoS Pathog 3, e27. doi:10.1371/journal.ppat.0030027, 07-PLPA-RA-0017 [pii]

Zhang S, Finkelstein A, Collier RJ (2004a) Evidence that translocation of anthrax toxin's lethal factor is initiated by entry of its N terminus into the protective antigen channel. Proc Natl Acad Sci U S A 101:16756–16761

Zhang S, Udho E, Wu Z et al (2004b) Protein translocation through anthrax toxin channels formed in planar lipid bilayers. Biophys J 87:3842–3849

Zhao Y, Yang J, Shi J et al (2011) The NLRC4 inflammasome receptors for bacterial flagellin and type III secretion apparatus. Nature 477:596–600. doi:10.1038/nature10510

Chapter 10
Staphylococcal β-barrel Pore-Forming Toxins: Mushrooms That Breach the Greasy Barrier

Jack Fredrick Gugel and Liviu Movileanu

Abstract *Staphylococcus aureus* exhibits a myriad of virulence elements, including β-barrel pore-forming toxins (β-PFTs). The primary mission of these protein toxins is to destroy the physical and chemical gradients across the membrane of the targeted cell by generating well-defined transmembrane pores, ultimately causing the cell death. Such a form of biomolecular attack is a ubiquitous membrane-perforation mechanism in numerous organisms, including bacterial systems and eukaryotes. One unusual commonality of the β-PFTs is their amphipathic nature, enabling sophisticated conformational alterations that are required for their transit from the secreting to attacked cell. Intriguingly enough, proteinaceous toxins are secreted as a hydrophilic form. Then, they must navigate within the aqueous phase between the two cells and ultimately breach the hydrophobic barrier posed by the susceptible cell membrane. The archetype of these non-enzymatic staphylococcal β-PFTs is the homoheptameric α-hemolysin (αHL) protein. Moreover, *S. aureus* has the ability to secrete up to four heteromeric, bi-component β-PFTs. Although the homomeric and heteromeric β-PFTs are related in sequence, homology, and structure, they demonstrate distinct biophysical features.

Keywords Unitary conductance • Polymer partitioning • Cysteine scanning mutagenesis • Bi-component toxin protein • Channel gating • Rational protein design • Subunit stoichiometry • Chemical modification

J.F. Gugel
Department of Physics, Syracuse University,
201 Physics Building, Syracuse, NY 13244-1130, USA

L. Movileanu (✉)
Department of Physics, Syracuse University,
201 Physics Building, Syracuse, NY 13244-1130, USA

Structural Biology, Biochemistry, and Biophysics Program, Syracuse University,
111 College Place, Syracuse, NY 13244-4100, USA

The Syracuse Biomaterials Institute, Syracuse University,
121 Link Hall, Syracuse, NY 13244, USA
e-mail: lmovilea@syr.edu

A.H. Delcour (ed.), *Electrophysiology of Unconventional Channels and Pores*,
Springer Series in Biophysics 18, DOI 10.1007/978-3-319-20149-8_10

10.1 What Do the β-PFTs Have and Not Have in Common?

Transmembrane protein pores represent cytotoxic factors expressed by various bacterial organisms, including *Escherichia coli*, *S. aureus*, *Bacillus cereus*, *Vibrio cholerae*, *Streptococcus pneumoniae*, and *Aeromonas hydrophila* (Parker and Feil 2005; Gonzalez et al. 2008; Iacovache et al. 2008; Bischofberger et al. 2009; Iacovache et al. 2010; Los et al. 2013). The focus of this book chapter is to provide a comprehensive overview of bacterial β-barrel pore-forming exotoxins (β-PFTs) secreted by *S. aureus* (Heuck et al. 2001; Menestrina et al. 2001, 2003; Comai et al. 2002; DuMont and Torres 2014; Iacovache et al. 2010; Otto 2014). This organism is a human pathogen that produces a number of β-PFTs. An interesting trait of these proteins is their ability to undergo complex structural transformations in such a way that they adapt to both the aqueous phase and hydrophobic environments. Therefore, these protein toxins cannot be placed into either the category of hydrophilic polypeptides or hydrophobic transmembrane proteins. In addition, the existence of such proteins questions the biophysical concept that a unique protein sequence determines a unique three-dimensional structure. This demonstrates that the nature of the bathing solvent is crucial for establishing the protein structure. The major commonality of these β-PFTs is that they are first synthesized as hydrophilic monomers, which then travel until they reach the membrane of the susceptible cell. The membrane represents a convenient environment for monomer attachment to a surface as well as oligomerization and pre-pore formation. The final step of these transformations is the pore formation within the hydrophobic membrane.

The structure of the pore is a β-barrel that spans the lipid membrane and is made by an even number of anti-parallel β-strands. The hydrophobic residues of the β-strands are oriented towards the external side (e.g., that of the lipid bilayer), whereas the hydrophilic side chains are oriented towards the β-barrel interior, conferring a hydrophilic environment for the transport of diverse water-soluble nutrients. Moreover, because the anti-parallel β-strands are connected through a network of numerous hydrogen bonds, the β-barrel structure shows an unusual mechanical, electrical and thermodynamic stability (White and Wimley 1999; Wimley 2003), an attribute that has been extensively used in membrane protein design (Bayley and Cremer 2001; Bayley and Jayasinghe 2004; Bayley et al. 2004; Kang et al. 2005; Jung et al. 2006; Howorka and Siwy 2008; Movileanu 2008, 2009; Howorka and Siwy 2009; Majd et al. 2010; Siwy and Howorka 2010; Mayer and Yang 2013).

We now know that β-PFTs are multimeric protein complexes. However, one feature that they do not share is the identity of the participating complex subunits: some toxins are homomeric, whereas others are heteromeric. An immediate example of the homomeric β-PFTs is the αHL protein pore (Song et al. 1996). The heteromeric β-PFTs contain two distinct polypeptides. That is why they are sometimes called bi-component β-PFTs (Ferreras et al. 1998; Pedelacq et al. 1999; Werner et al. 2002; Sugawara-Tomita et al. 2002; Menestrina et al. 2003; Potrich et al. 2009; Yamashita et al. 2011). Therefore, there must be different kinetics and dynamics of the complex formation of these proteins. This is schematically illustrated below.

$$\alpha_1^{u} \rightarrow \alpha_1^{b} \rightarrow \alpha_1^{b^*} \rightarrow \alpha_7^{pp} \rightarrow \alpha_7^{p} \quad (10.1)$$

$$\alpha_1^{u} + \beta_1^{u} \rightarrow \alpha_1^{b} + \beta_1^{u} \rightarrow (\alpha_1\beta_1)^{b} \rightarrow (\alpha_1\beta_1)^{b^*} \rightarrow (\alpha_n\beta_n)^{pp} \rightarrow (\alpha_n\beta_n)^{p} \quad (10.2)$$

On the top row, the steps of oligomerization and pore formation of the αHL protein are shown (Scheme 10.1). α_1^{u} indicates a membrane-unbound, water-soluble αHL monomer. α_1^{b} is a membrane-bound αHL monomer, whereas $\alpha_1^{b^*}$ is a membrane-bound αHL monomer in an activated conformation, a state that precedes the nonlytic formation of the homomeric αHL pre-pore (α_7^{pp}). The final state is the insertion of the stem domain of the homomer into the lipid bilayer of the susceptible cell, generating a transmembrane β-barrel protein pore (α_7^{p}). In contrast, the kinetics of pore formation of a bi-component β-PFT undergoes a more complex scheme (the bottom row, Scheme 10.2). Both types of bi-component toxin monomers are secreted as a hydrophilic form (α_1^{u} and β_1^{u}). Then, they navigate to the membrane of the susceptible cell. One class of monomers shows specific interactions with the membrane (α_1^{b}) before the heterodimerization at the membrane surface ($(\alpha_1\beta_1)^{b}$). This is followed by the reorientation of the heterodimer in an activated conformation ($(\alpha_1\beta_1)^{b^*}$) that enables the pre-pore formation ($(\alpha_n\beta_n)^{pp}$). Finally, an insertion of the stem into the membrane generates a transmembrane β-barrel pore of a bi-component β-PFT ($(\alpha_n\beta_n)^{p}$). The steps that lead from the unbound monomer to the insertion of a transmembrane protein pore are likely closely similar for all β-PFTs, as shown above. Such similarity suggests that they form a unique protein superfamily, including β-PFTs produced by other bacterial systems. Examples are aerolysin of *A. hydrophila*, cytolysin of *V. cholera*, *B. cereus* hemolysin II, and others. However, neither homomeric nor heteromeric β-PFTs of *S. aureus* include an enzymatic domain, such as in the case of the protective antigen of the anthrax toxin.

10.2 α-Hemolysin (αHL) is an Archetype of the Homomeric β-PFTs

It is likely that the most known β-PFT is staphylococcal αHL protein (Song et al. 1996; Gouaux 1998; Menestrina et al. 2001, 2003; Montoya and Gouaux 2003). This is a well-studied toxin because it exhibits virulence activity on a broad variety of mammalian cells, such as granulocytes and erythrocytes (Los et al. 2013). Such a protein complex is secreted as a water-soluble, 293-residue monomer, but it does assemble as a heptamer on model and cell membranes (Gouaux et al. 1994; Song et al. 1996; Cheley et al. 1997; Fang et al. 1997; Krasilnikov et al. 2000) (Table 10.1). The heptamer is a mushroom-shaped protein complex, in which each subunit contributes two anti-parallel β strands to the formation of the 14-stranded β barrel (Fig. 10.1a). The structure of the αHL protein is divided into three distinct domains: stem, rim, and cap. The cap domain, whose external diameter is ~100 Å, is located within the aqueous phase. The overall length of the complex from one opening to the other is ~100 Å, out of which the β-barrel domain (the stem domain) measures ~52 Å.

Table 10.1 Structural features of staphylococcal β-PFTs

Protein	Monomer mass (kDa)	Oligomer size	Available 3D structure	Barrel diameter (Å)	Barrel length (Å)	Lumen length (Å)
α-Hemolysin (αHL)	33.2	Homoheptamer (14 β strands)[a] Homohexamer (12 β strands)[b]	Detergent-solubilized heptamer[c]	26[c]	52[c]	100[c]
Leukocidin (Luk) LukF LukS	34 33	Hetero-octamer (16 β strands)[d]	NA[e]	NA[e]	NA[e]	NA[e]
γ-Hemolysin (γHL) LukF Hlg2	34 32	Hetero-heptamer (14 β strands)[f] Hetero-octamer (16 β strands)[g]	Detergent-solubilized octamer[g]	25.5[g]	47[g]	93[g]

[a]Gouaux et al. (1994); Song et al. (1996); Cheley et al. (1997); Fang et al. (1997); Krasilnikov et al. (2000)
[b]Under some experimental contexts, the αHL protein forms a hexameric structure (Czajkowsky et al. 1998)
[c]Song et al. (1996)
[d]Miles et al. (2002b); Jayasinghe and Bayley (2005)
[e]Not available
[f]Sugawara-Tomita et al. (2002)
[g]Yamashita et al. (2011)

The internal diameter of the barrel, excluding the side chains of the internal residues, is ~26 Å (Fig. 10.1b). However, if we include the side chains of the residues within the pore lumen, αHL exhibits a strongly varying internal diameter from ~16 Å, within the constricted region of the β barrel, to ~46 Å, within the cap domain. The average internal diameter of the β-barrel is ~20 Å.

It is quite interesting that almost the entire structure of the staphylococcal αHL protein is made of anti-parallel β strands, conferring an unusual mechanical, electrical and thermal stability. We will discuss below the critical importance of this trait, which has been heavily used for the transformation of the area of single-molecule biophysics. The heptameric structural organization is not challenged, as this has been determined either directly or indirectly by several independent approaches under various experimental contexts. The high-resolution, X-ray structure of the detergent-solubilized αHL protein revealed its heptameric structure (Song et al. 1996) (Fig. 10.1).

Collaborative efforts between Hagan Bayley's and Jie Yang's groups have produced an unquestionable demonstration that the αHL protein pore assembles as a heptamer (Cheley et al. 1997; Fang et al. 1997). Using atomic force microscopy (AFM) imaging of a β barrel-truncation αHL mutant, they showed that the stoichiometry of αHL remains heptameric even under the experimental contexts of the AFM approach (Fig. 10.2). Later, a high-impact methodology was developed by coupling chemical modification, protein engineering, SDS-PAGE gel analysis, and single-channel electrical recordings. In this case, targeted, engineered, or chemically-modified

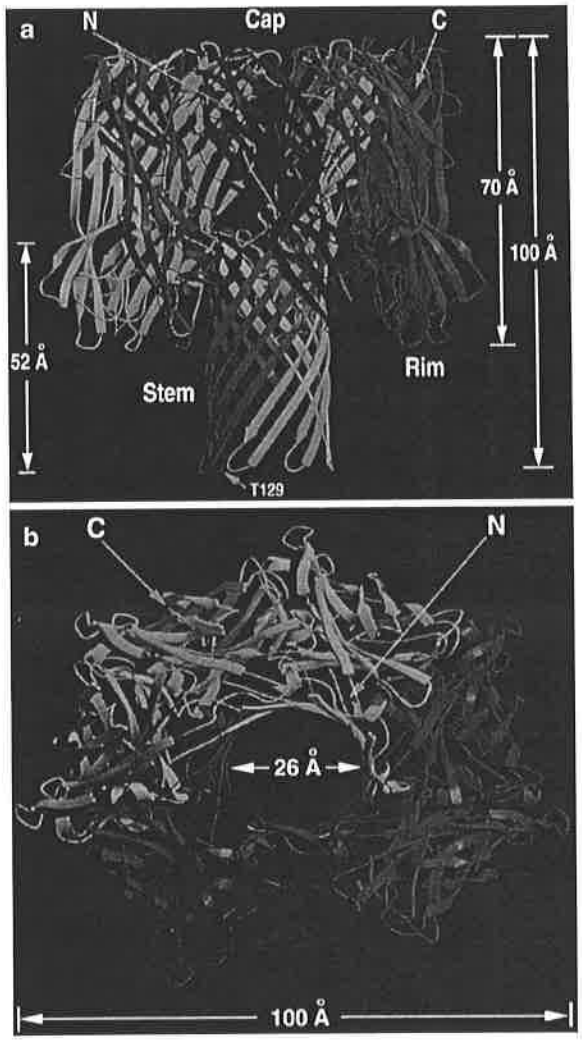

Fig. 10.1 αHL is presented using a ribbon representation. Here, individual protomers are illustrated by different colors. **(a)** This is a side view that is parallel to the putative lipid membrane; **(b)** This is a top view. It reveals the seven-fold symmetry of the protein. The αHL protein model was generated using 7ahl.pdb (Reproduced, with permission, from reference (Song et al. 1996))

αHL heteromers were separated and visualized as resulting protein band products of combinations and permutations of the unmodified and native subunits of a heptameric protein (Braha et al. 1997; Howorka et al. 2000; Movileanu et al. 2000). Single-channel electrical recordings and analysis permitted the obtaining of informative data pertinent to the desired heteromers. These spectacular experiments were only possible owing to a great feature of this protein: its stability in SDS up to 65 °C, a stunning

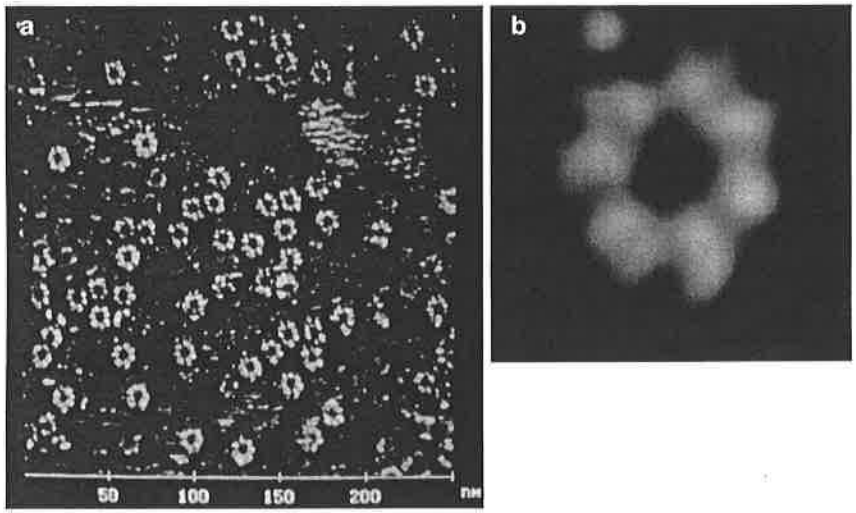

Fig. 10.2 The use of atomic force microscopy (AFM) imaging to show that the αHL protein pore is a homoheptameric β-PFT. (**a**) An αHL mutant, made by truncation of the native β-barrel, was attached on an AFM mica grid as a heptamer. The horizontal scale bar is marked in nanometers; (**b**) An AFM image of an individual β-barrel truncation αHL mutant (Reproduced, with permission, from reference (Cheley et al. 1997))

discovery made at an earlier time (Walker and Bayley 1995). Later in this chapter, we show that this exceptional feature has also been employed to determine the subunit composition of a bi-component β-PFT (Miles et al. 2002b).

Moreover, Krasilnikov and coworkers (Krasilnikov et al. 2000) demonstrated that the αHL protein is a heptamer under experimental contexts of reconstitution into a planar lipid bilayer. They used targeted cysteine mutagenesis, sulfhydryl-directed reagents, and single-channel electrical recordings (Sackmann and Neher 1995). Each chemical reaction between an engineered cysteine sulfhydryl and a sulfhydryl-directed reagent molecule produced a distinctive current blockade. A total of seven reagent-induced current blockades were noted during the same single-channel experiment, confirming the heptameric structure of αHL. We will show below that such a methodology worked well for the determination of the subunit composition of a staphylococcal bi-component β-PFT (Miles et al. 2002b).

10.3 Why Did αHL Become Such a Popular Transmembrane Protein Pore?

Speaking about staphylococcal αHL protein pore in a book chapter raises our obligation to provide a clear message to a non-expert reader that protein biochemistry and electrophysiological studies involving this protein have transformed the area of single-molecule biophysics. In addition, extensive studies using αHL impacted our

understanding of membrane protein folding, stability, and design. Moreover, αHL was heavily utilized in studies of bionanotechnology (Majd et al. 2010), particularly with implications in high-resolution DNA (Astier et al. 2005; Bayley 2006; Branton et al. 2008) and protein (Movileanu 2009; Mayer and Yang 2013) detection and analysis. Therefore, it is impossible to mention all of the outstanding articles involving this protein. However, it needs to be said that such major αHL-related transformations in these rapidly changing areas were primarily driven by many of the advantageous characteristics of this protein. The single-channel conductance of αHL is ~260 pS and 960 pS in 300 mM KCl (Howorka et al. 2000) and 1000 M KCl (Movileanu et al. 2003), respectively (Table 10.2). The αHL protein pore is weakly anion selective ($P_{Cl}/P_K = 1.5$, pH 7.0) (Menestrina 1986), exhibiting gating fluctuations at low, physiological salt concentrations (Mohammad and Movileanu 2010) and acidic pH (Kasianowicz and Bezrukov 1995; Mohammad et al. 2012). This protein self-assembles on planar lipid bilayers into a single orientation (Menestrina 1986; Bezrukov and Kasianowicz 1993).

The αHL pore maintains its quiet, large-conductance open state for long periods of time even under extreme conditions of pH (from 4 to 11) (Gu and Bayley 2000; Misakian and Kasianowicz 2003), transmembrane potential (Menestrina 1986; Korchev et al. 1995), temperature (up to 95 °C) (Kang et al. 2005; Jung et al. 2006), salt concentration (several molar) (Bezrukov et al. 2004; Rodrigues et al. 2008) or osmotic pressure (a few tens of % (w/v) PEGs) (Bezrukov et al. 1996; Krasilnikov and Bezrukov 2004; Gu et al. 2003). The transport processes of molecules across this protein pore can be readily designed and implemented, by imposing different thermodynamic driving forces for the translocating molecules, such as transmembrane potentials, transmembrane difference in pH, ionic strength, disulfide-thiol

Table 10.2 Electrophysiological traits of staphylococcal β-PFTs

Protein	Conductance (pS)	Ion Selectivity	Permeability ratio (P_K/P_{Cl})
α-Hemolysin (αHL)	260[a] 960[b] 92[c]	Weakly anion-selective	0.6[c] 0.8[d]
Leukocidin (LukF/LukS)	2540[d]	Weakly cation-selective	1.7[e]
γ-Hemolysin (γHL)			
HlgA/HlgB	115[f]	Weakly cation-selective	1.3[g]
HlgC/HlgB	192[f]		3.6[g]

[a]This value was determined in 300 mM KCl, 5 mM Tris.HCl, pH 7.0 (Howorka et al. 2000)
[b]This value was determined in 1000 mM KCl, 10 mM Tris.HCl, pH 7.5 (Movileanu et al. 2003)
[c]This value was determined in 100 mM NaCl, pH 7.0 (Menestrina 1986)
[d]This value was determined in 1000 mM KCl, 5 mM HEPES, pH 7.4 (Miles et al. 2001)
[e]These values were determined when the *cis* and *trans* chambers contained 1000 mM and 200 mM KCl, respectively. The buffer solution contained 5 mM HEPES, pH 7.4. The *cis* chamber was grounded (Miles et al. 2001)
[f]This value was determined in 100 mM NaCl, 20 mM HEPES, pH 7.0 (Comai et al. 2002)
[g]These values were determined when the chambers contained 20 (*cis*) and 200 (*trans*) mM KCl, respectively. The buffer solution contained 20 mM HEPES, pH 7.0. The *cis* chamber was grounded (Comai et al. 2002)

exchange or other physical and chemical gradients, as both sides of the membranes are fully accessible in a planar lipid membrane format. It was found that αHL may serve as a permeation pathway for a broad range of molecules, including highly flexible and neutral PEGs of up to ~3 kDa (Bezrukov et al. 1996; Movileanu et al. 2001; Movileanu and Bayley 2001; Krasilnikov and Bezrukov 2004; Krasilnikov et al. 2006), positively charged peptides (Movileanu et al. 2005; Sutherland et al. 2005), negatively charged single stranded RNAs and DNAs of greater molecular mass (~ tens of kDa) (Kasianowicz et al. 1996; Akeson et al. 1999; Meller et al. 2000), and large proteins in unfolded conformation (Rodriguez-Larrea and Bayley 2013; Nivala et al. 2013). In addition, the αHL pore interacts with cyclodextrins (Gu et al. 1999, 2003), cyclic peptides (Sanchez-Quesada et al. 2000), and crown ethers (Bezrukov et al. 2004), some of which were used as molecular adapters for the design and creation of various molecular biosensors. Later, αHL was used to obtain a mechanistic understating of the binding interactions between enzymes and DNA (Hornblower et al. 2007; Benner et al. 2007), with great expectations for DNA sequencing (Bayley 2006; Branton et al. 2008; Cherf et al. 2012). The use of αHL in polymer translocation studies stimulated a new realm called *nanopore biophysics*. For example, the current blockades induced by polymer partitioning into a single αHL protein pore were indicative of the polymer properties, which included the polymer length, persistence length, repetitive unit composition, and secondary structure. Moreover, these single-channel parameters strongly depended on other physical traits of the lipid bilayer-pore system, such as temperature, transmembrane potential, ionic strength, pH, and osmotic pressure. Therefore, it is not surprising that such fundamental polymer-pore studies were rapidly extended to applicative areas of bionanotechnology (Bayley et al. 2004; Bayley and Jayasinghe 2004; Maglia et al. 2008, 2009; Hall et al. 2010; Wang et al. 2011, 2013a, b; Gurnev and Nestorovich 2014; Kusters et al. 2014).

In Fig. 10.3a, we illustrate the sites at which native residues were substituted by cysteines. Systematic examinations of the chemical reactions between sulfhydryl-directed PEGs and individual cysteine residues have provided information on both the single polymer dynamics under confined nanopore environment (Howorka et al. 2000; Movileanu et al. 2000; Movileanu and Bayley 2001) as well as the internal geometry of the pore interior (Bezrukov 2000; Movileanu et al. 2001). A wealth of theoretical and computational studies was already available at that time (Muthukumar 1999; De Gennes 1999a, 1999b, 1999c; Brochard-Wyart et al. 2000). Later, more extensive theoretical examinations were stimulated by experimental studies using single αHL protein nanopores (Slonkina and Kolomeisky 2003; Tian and Andricioaei 2005; Kong and Muthukumar 2005; Kolomeisky 2007; Goodrich et al. 2007; Muthukumar 2007; Kolomeisky 2008; Maffeo et al. 2012). These experimental studies have provided a new methodology for the systematic exploration of the lumen of the transmembrane protein pores. In addition, such experiments have enabled the direct determination of the number of subunits of a desired cysteine αHL mutant that interact with a specific polymer of a given size (Movileanu et al. 2003).

For example, a single-channel trace acquired with $T117C_7$, a homoheptamer cysteine αHL mutant (Fig. 10.3a), is shown in Fig. 10.3b, c. When a sample of sulfhydryl-directed PEG-1 kDa was applied to the chamber, brief current blockades

were observed, representing transient movements of the polymer into the nanopore interior. This pattern was followed by a permanent current blockade (Fig. 10.3b, state 1), which indicated that one sulfhydryl-directed PEG-1 kDa covalently reacted with a cysteine sulfhydryl. The amplitude of the transient current blockades was comparable with the amplitude of the permanent current blockade, suggesting that indeed a single PEG-1 kDa produced a current blockade, whose size corresponds to 2/3 that of the unitary conductance of the αHL protein pore. Again, the open state 1

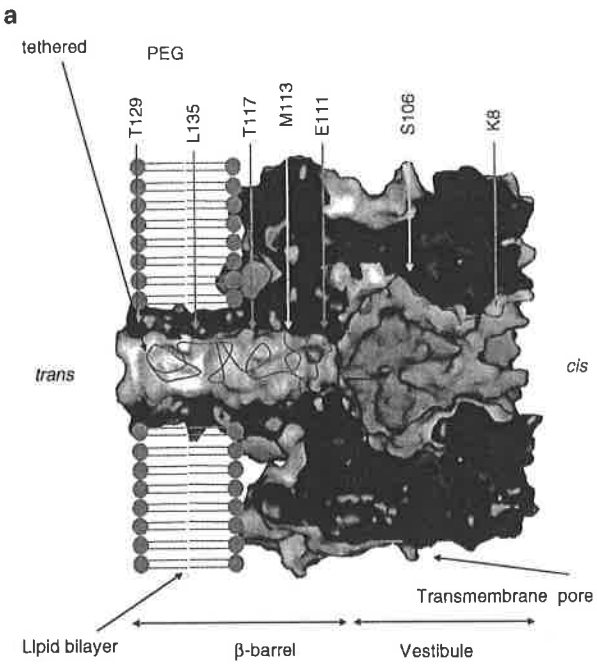

Fig. 10.3 Examples of single-channel electrical recordings monitoring single-molecule chemical reactions of individual sulfhydryl-directed PEGs-1 kDa reagent with a cysteine αHL mutant. (**a**) Cross-sectional view of the αHL protein pore illustrating sites where single cysteines were engineered for the exploration of polymer partitioning. The partitioning of poly(ethylene glycol)s (PEGs) of different sizes was examined by covalent modification of the pore lumen. The chemical reaction occurred between the reactive sulfhydryl-containing group of the PEG and the individual cysteine sulfhydryl of each reconstituted αHL mutant. Seven cysteine αHL mutants were examined at the locations labeled in the figure; (**b**) The cysteine was engineered within the β-barrel region of the pore, in position T117. This single-channel current resulted from voltage-induced ion translocation through the pore. The trace indicates permanent current blockades produced by individual, reacted polymers with cysteine sulfhydryls. Two distinguished permanent current blockades showed that two independent polymers reacted with distinct cysteine sulfhydryls within the pore lumen; (**c**) Application of the reducing agent to the chamber facilitated the cleavage of both PEGs from the pore lumen, producing a full recovery of the unitary conductance of αHL. In (**B**) and (**C**), the buffer solution contained 1 M KCl, 10 mM Tris.HCl, and 100 μM EDTA, pH 8.5. The applied transmembrane potential was +100 mV. The single-channel electrical traces were low-pass Bessel filtered at 10 kHz (Reproduced, with permission, from references (Movileanu et al. 2003) and (Movileanu and Bayley 2001). Copyright © (2001) National Academy of Sciences, U.S.A)

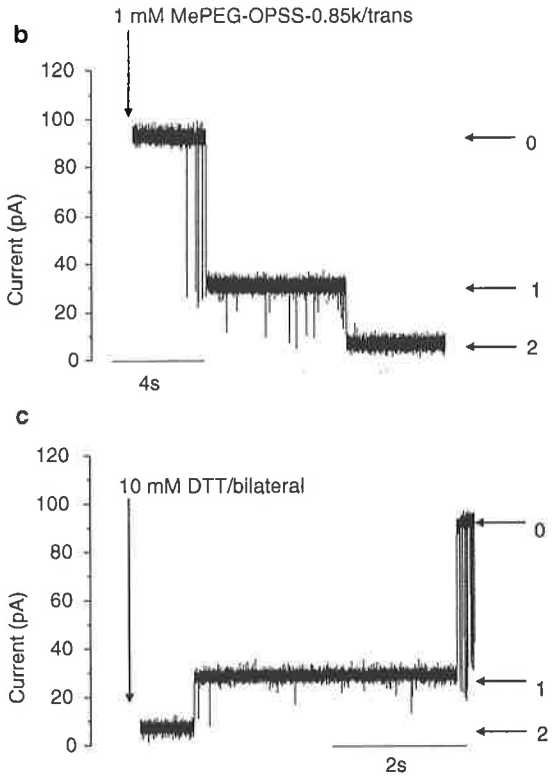

Fig. 10.3 (continued)

was accompanied by short-lived current spikes and followed by a second permanent current blockade (Fig. 10.3b, state 2), which indicated that a second polymer reacted with a cysteine sulfhydryl. Therefore, only two PEGs-1 kDa were accommodated at position T117C. These single covalent reactions were reversed upon addition of the reducing agent to the chamber (Fig. 10.3c). This example revealed the informative power of single-channel electrical recordings of the modified αHL protein pore, providing a clear indication on what is the total molecular size of the sulfhydryl-directed PEGs reacted at a desired location. Why would the two types of current blockade events have different amplitudes? The first reacted polymer reduced the ionic flux about 2/3 of that corresponding to the unitary conductance, whereas the second reacted polymer altered the ionic flux about 1/3 of that corresponding to the unitary conductance. This distinction might be determined by a difference in the local conformation of the reacted PEGs-1 kDa. Another possibility was that only a fraction of the second reactive polymer partitioned into the pore lumen, leaving the remaining fraction outside the pore.

PEGs produced a longer current blockade through the αHL protein pore lumen at increased salt concentrations, likely owing to electro-osmotic effect (Krasilnikov et al. 2006; Rodrigues et al. 2008). Taking into account this finding, John Kasianowicz and

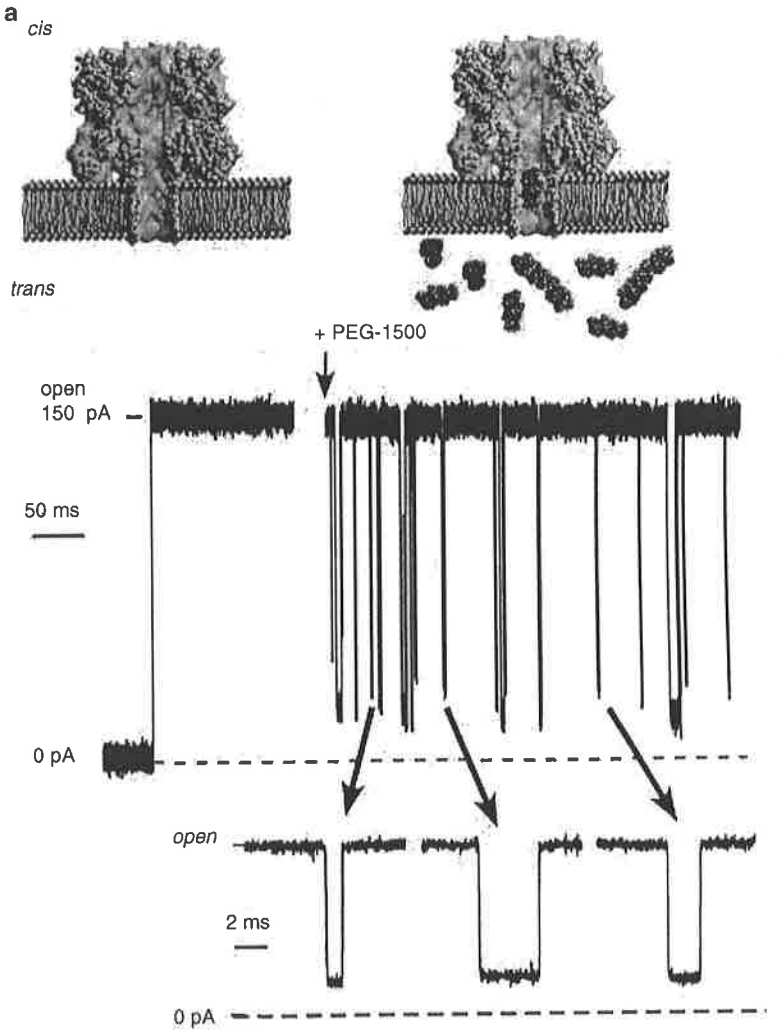

Fig. 10.4 Development of single-molecule mass spectrometry using a single protein nanopore. (**a**) The αHL protein pore was inserted into a planar lipid bilayer, enabling a quiet single-channel current. Application of a sample of polydisperse PEG to the chamber produced well-defined current blockages, the nature of which depended on the length of the PEG molecules as well as their concentration. The horizontal dashed lines show the level of the zero current; (**b**) A single αHL protein nanopore can be used to resolve the monodisperse (mPEG; with a molecular weight of 1.3 kDa; lower panels) and polydisperse (pPEG; with a molecular weight of 1.5 kDa; upper panels) PEG samples. The standard histograms of the current amplitudes indicated either a single, broad distribution (the top panel) or two well-separated and narrow distributions (the bottom panel). The buffer solution contained 4 M KCl, 5 mM Tris, pH 7.5. The applied transmembrane potential was +40 mV. In the bottom trace of (**b**), the peak given by the long-lived current blockades was interpreted in terms of impurities present in the mPEG sample (Reproduced, with permission, from reference (Robertson et al. 2007). Copyright © (2007) National Academy of Sciences, U.S.A)

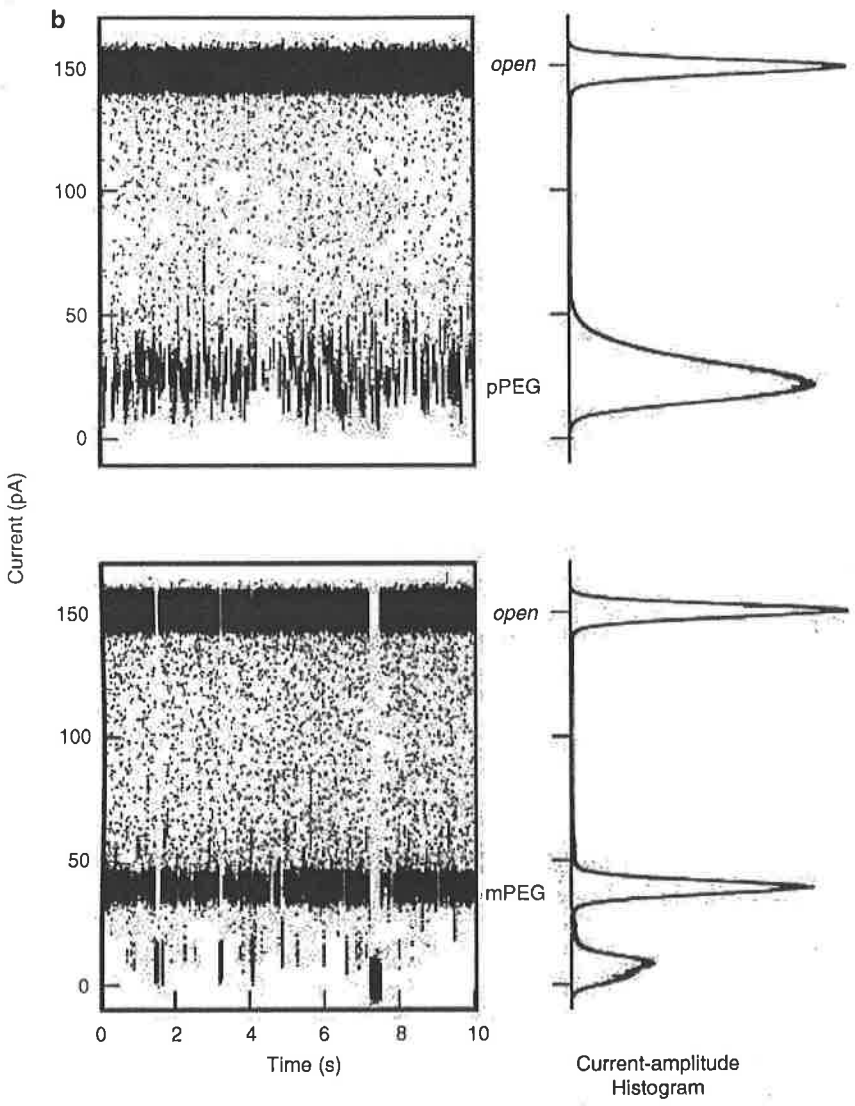

Fig. 10.4 (continued)

co-workers have developed an elegant nanopore-based, single-molecule mass spectrometry for sizing flexible polymers in solution (Robertson et al. 2007, 2010; Reiner et al. 2010; Baaken et al. 2011). The stunning discovery was that, under experimental conditions of high salt concentration, PEG molecules produced distinctive mass-dependent transient current blockades when they partitioned into the αHL protein pore.

In Fig. 10.4a, a quiet single-channel current is shown in the absence of PEG, but frequent and reversible current transitions were observed in the presence of PEGs added to the chamber. A very high salt concentration in the chamber was advantageously used

for both increasing signal-to-noise ratio due to increase in the unitary conductance and prolonging the residence times due to local osmotic pressure on trapped PEGs into the pore lumen. In Fig. 10.4b, the top trace shows the open-state current and current blockades of varying amplitude made by a polydisperse sample of PEG (pPEG), whereas the bottom trace indicate uniform current blockades produced by a monodisperse sample of PEG (mPEG). In contrast to Fig. 10.4a, the time scale is compressed, so that the current blockades cannot be observed in full in Fig. 10.4b. In addition, all inter-event intervals, otherwise distinguishable in Fig. 10.4a, were removed in Fig. 10.4b. Such a single-channel electrical trace representation enabled an easier determination that the pPEG histogram distribution is noisier than that acquired with mPEG. pPEG sample contained a mixture of polymer molecules with a number of repetitive units varying from 25 to 50. However, average molecular weight of pPEG was similar to that of mPEG. There is a clear distinction between the results obtained with mPEG and pPEG. The current-amplitude histograms demonstrated a single and broad distribution with pPEG. In contrast, the current-amplitude histogram obtained with mPEG revealed two narrower distributions. The second level of the current blockades, given by the long-lived events, in the experiment using mPEG, was interpreted in terms of impurities in the PEG sample. Using the mean current value of each blockade, histograms with multiple current-blockade distributions correlated with multiple molecular-mass PEGs, demonstrating the informative power of these measurements for discriminating various PEGs within the same sample.

Remarkably, this method has proven the ability to resolve the repetitive unit of PEG, which was beyond the previous attempts (Bezrukov et al. 1996; Movileanu et al. 2003). The residence time of PEG within the pore lumen was increasing with the increase in the molecular mass of PEG in a monotonic fashion. It was also demonstrated that sizing and discriminating analytes in real time can be accomplished in the case of neutral polymeric species. We do not anticipate challenges in applying this methodology for other neutral, water-soluble and flexible polymers. Modelling the transient current blockades as signal responses given by an equivalent electrical circuit has permitted an additional level of analysis of analyte-produced events, increasing the resolution of the residence times produced by flexible polymers and open sub-states at sub-picoampere level (Balijepalli et al. 2014). Finally, it is worth mentioning that all traits of the αHL protein pore ignited persistent interest of computational biophysicists in the modeling of ion transport across channels and pores, a primary goal of modern electrophysiology (Noskov et al. 2004; Aksimentiev and Schulten 2005; Wells et al. 2007).

10.4 Structural Properties of Leukotoxin Monomers

S. aureus secretes not only homomeric, but also heteromeric β-PFTs. For example, a mandatory interaction between two distinct monomers, one that is part of the class F polypeptides and one that belongs to the class S polypeptides, results in the formation of heteromeric or bi-component β-PFTs. They include leukocidins (Luk), γ-hemolysins (γHL), and Pantom-Valentine leukocidins (PVL) (Ferreras et al. 1998;

Olson et al. 1999; Pedelacq et al. 1999; Prevost et al. 2001; Sugawara-Tomita et al. 2002; Guillet et al. 2004; Yoong and Torres 2013; Alonzo and Torres 2014). No experimental evidence is available on direct interactions between two similar monomers of class F or two similar monomers of class S. Therefore, homomeric β-PFTs containing either class F or class S polypeptides have never been detected. Because each class of leukotoxin polypeptides includes several members, four bi-component β-PFTs have been determined so far (Yoong and Torres 2013; Alonzo and Torres 2014). PVL complexes are formed by LukS-PV and LukF-PV subunits. The γHL protein pores are made by either HlgA and HlgB subunits or HlgC and HlgB subunits (Comai et al. 2002). LukED leukotoxins consist of LukE and LukD polypeptides. LukAB/LukGH toxins are made by either LukA and LukB or LukH and LukG.

The diversity of bi-component β-PFTs is also consistent with their distinctive lytic activities with respect to various cell membrane models (Yoong and Torres 2013; DuMont and Torres 2014; Alonzo and Torres 2014). All four types of leukocidins produce the death of human neutrophils, whereas only LukED and γHL induce lysis against erythrocytes (Yoong and Torres 2013). The mechanisms by which the individual monomers bind to the cell membrane surface, then oligomerize and assemble into a transmembrane β-barrel protein pore are not yet completely understood. These bi-component β-PFTs efficiently assemble on lipid membranes either in the absence (Miles et al. 2001, 2002b; Jayasinghe and Bayley 2005; Holden et al. 2006) or presence of cellular receptors located on the surface of the susceptible cells (Yoong and Torres 2013; DuMont and Torres 2014; Alonzo and Torres 2014).

In Fig. 10.5, we illustrate the relationships among the polypeptides of the homomeric and heteromeric β-PFTs. The sequence identity of the members of either class with that of αHL is always less than 30 %. There is an increased sequence identity among the members within the same class: 71–79 % and 59–79 % for the class F and S polypeptides, respectively (Gouaux et al. 1997). The X-ray crystal structure of LukF reveals that its fold looks closely similar to that of the αHL protomer in the heptameric complex, except for two domains that are intimately involved in the protomer-protomer contacts and in the binding of the monomer to the membrane surface (Olson et al. 1999). These are the amino latch and pre-stem domains and they are involved in the protein-protein and protein-membrane interfaces, respectively. Parallel studies by Pédelacq and colleagues revealed an almost identical fold of the water-soluble LukF-PV polypeptide (Pedelacq et al. 1999). Later, the same group was able to determine the structure of the water-soluble LukS-PV polypeptide at 2.0 Å resolution (Guillet et al. 2004). Interestingly, it was found that the overall structure of LukS-PV is identical to that of the water-soluble LukF monomer and the αHL protomer, except for the domain that interfaces its interaction with the lipid membrane (the rim domain, Fig. 10.1a). This finding suggested a different propensity of LukS-PV to interact in a distinct fashion with the membrane surface of the susceptible cells.

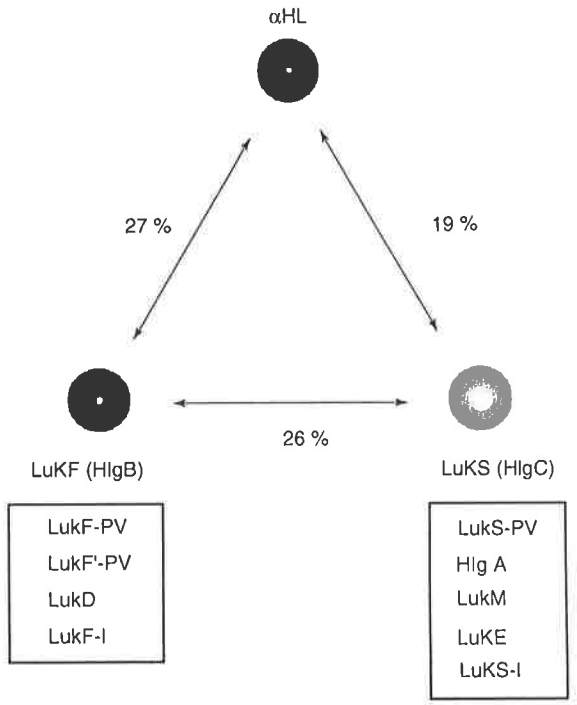

Fig. 10.5 Residue sequence relationships among αHL, LukF (HlgB), and LukS (HlgC). The boxes indicate other components of the F and S classes of the staphylococcal bi-component β-PFTs. HlgA, HlgB, and HlgC are polypeptides corresponding to γHL (Reproduced, with permission, from Reference (Miles et al. 2002b))

10.5 Electrophysiological Traits of the Staphylococcal Bi-component β-PFTs

Based on similarities in protein folding between each of the leukotoxin monomers with the αHL protomers (Olson et al. 1999; Pedelacq et al. 1999; Guillet et al. 2004), the staphylococcal bi-component β-PFTs were expected to form large-conductance pores in all model and cell membranes. In accord with this anticipation, Miles and colleagues found that the bi-component Luk protein complex (LukF/LukS) forms transmembrane pores on planar lipid membranes with a single-channel conductance of ~2540 pS in 1000 mM KCl, 5 mM HEPES, pH 7.4 (Table 10.2) (Miles et al. 2001). The single-channel conductance of the LukF/LukS protein pore is ~3-fold greater than that of the αHL protein pore. The value of the unitary conductance of the heptameric hemolysin II, a β-PFT of *B. cereus*, measured under similar experimental contexts, is 630 pS (Miles et al. 2002a). A large difference between the single-channel conductance of the LukF/LukS and αHL protein pores or the LukF/LukS and *B. cereus* hemolysin II protein pores suggested that the number of participating subunits to the LukF/LukS protein pore complex is greater than that corresponding to the homomeric β-PFTs.

Moreover, systematic measurements of the reversal potentials under various ionic gradients have revealed that the LukF/LukS pores represent weakly cation

selective pathways across the lipid bilayers (Table 10.2). This weak cation selectivity is surprising, given the lack of negative charges within the narrowest region of the lumen, the β-barrel part of the pore, except for a single residue, Asp-122 of LukF. Another mechanism of this selectivity might be the cluster of acidic residues within the cap domain, facing the opening of the pore and in the proximity of the N-termini of both LukF and LukS polypeptides (Comai et al. 2002). Such negatively charged residues do not exist within the same location of the αHL polypeptide. The LukF/LukS protein pores exhibit voltage-induced current gating at positive transmembrane potentials greater than 60 mV, and in 1000 mM KCl, 5 mM HEPES, pH 7.4, but a remarkable stability of the open-state current at large negative applied transmembrane potentials (e.g., 120 mV or greater than this value). Again, this is in contrast to αHL protein pore, whose open-state current remains stable for long periods at positive applied potentials up to +160 mV, but undergoes gating fluctuations at negative applied transmembrane potentials greater than 100 mV (Movileanu et al. 2005). It might be possible that the gating mechanisms of the two β-PFTs are different. In the case of the αHL protein, brief current flickering at positive potentials and at low, physiological salt concentrations are likely caused by the localized fluctuations of the structurally flexible glycine-rich turn of the β-barrel domain of the pore (Mohammad and Movileanu 2010).

Extensive studies on other leukotoxins have confirmed increased unitary conductance and weak cation selectivity. For instance, Comai and colleagues determined that γHLs, consisting of either HlgA/HlgB or HlgC/HlgB, exhibit a unitary conductance of either 115 or 192 pS, respectively, in 100 mM NaCl (Table 10.2) (Comai et al. 2002). These values are greater than that measured with αHL under similar experimental conditions (~92 pS) (Menestrina 1986). Using PEGs in osmotic-protection experiments, the effective pore diameter of γHLs was 20–24 Å (Ferreras et al. 1998). The above-mentioned hypothesis that the weak cation selectivity is produced by a cluster of acidic residues located within the cap domain near the pore opening was confirmed by single- and multiple-site mutagenesis (Comai et al. 2002). Indeed, by engineering charge-reversal mutations of negative → positive charge, namely converting all acidic side chains of the cluster into basic residues, the unitary conductance and ion selectivity of αHL were obtained. Therefore, this cluster of negative charges in γHLs represents a selectivity filter.

10.6 Subunit Composition of Staphylococcal Bi-component β-PFTs

Given extensive biochemical and biophysical studies employing staphylococcal bi-component β-PFTs, along with detailed structural information about the leukotoxin oligomers, one would immediately ask what is the subunit stoichiometry of the protein pore complex? Because the single-channel conductance of the LukF/LukS protein complex is about three times greater than that of αHL (Miles et al. 2002b), it is likely that the number of participating subunits of the LukF/LukS protein

complex is greater than seven. Heteromeric composition of the LukF/LukS protein complex has been addressed using two independent methodologies: (i) gel-shift electrophoresis assay, and (ii) single-channel electrical recordings, along with chemical modification at strategic locations of the pore interior (Miles et al. 2002b).

In the first approach, individual LukF and LukS polypeptides were fused to the C-terminal, 94-residue extension of the *B. cereus* hemolysin II (TL). Other β-PFTs lack this C-terminal extension. The primary motivation for this protein design was the TL-induced alteration of the gel-shift mobility of the LukF and LukS polypeptides could be noted on an SDS-PAGE gel. This strategy was coupled with the structural stability of the oligomers in SDS-PAGE gels. Such an approach enabled the *in vitro* transcription and translation (IVTT) of the protein complex assembled on rabbit red blood cell membranes (rrbcm), and then SDS-PAGE gel separation of the engineered heteromer complexes containing subunits with or without TL. In this way, various heteromers containing either LukF-TL and LukS subunits or LukF and LukS-TL subunits were resolved on the SDS-PAGE gels.

For example, in the first experiment heteromers containing various ratios of wild-type LukF (WT LukF) and LukF-TL with wild-type LukS (WT LukS) were produced by cotranslation in the presence rrbcm. Bands with increments in electrophoretic mobility were observed. Four new bands were observed in addition to the band corresponding to WT LukF/WT LukS. The fastest band was attributed to WT LukF/WT LukS. The TL-induced, slow-mobility bands were produced by heteromers with either one, two, three, or four LukF-TL subunits. This finding indicated that the LukF/LukS protein complex contains four LukF subunits. In the second experiment, a similar approach was employed to examine the contribution of LukS to the heteromeric complex. It was determined that LukF/LukS contains four LukS subunits as well. In brief, such gel-shift electrophoresis assay on SDS-PAGE gels, along with protein design, indicated that the LukS/LukF protein complex is an octamer.

In the second approach, targeted chemical modification of engineered cysteines within the pore lumen, along with single-channel electrical recordings were employed (Fig. 10.6). To some extent, this second approach was quite related to the previous test. This is becuase the gel-shift assay used for the engineered heteromers was replaced by the unitary conductance change produced by individual chemical reactions of a sulfhydryl-specific reagent sodium (2-sulfonatoethyl)methanethiosulfonate (MTSES) molecule with an engineered cysteine sulfhydryl of a Luk polypeptide within the complex (either LukF or LukS). These studies proved that both LukF-S124C/WT LukS and WT LukF/LukS-A122C underwent four distinct current blockades when MTSES was applied to the bilayer chamber. Recovery of the unitary conductance was achieved by the addition of the DTT reducing reagent. This conductance recovery was observed in the form of four step-wise current upshifts, suggesting that the LukS/LukF protein complex is an octamer.

Independently of and in parallel with these studies, Sugawara-Tomita and colleagues, using high-resolution electron microscopy and chemical cross-linking experiments, discovered that γHL assembles in a stochastic fashion as a heptamer of either 4 LukF subunits and 3 Hlg2 subunits or 3 LukF subunits and 4 Hlg2 sub-

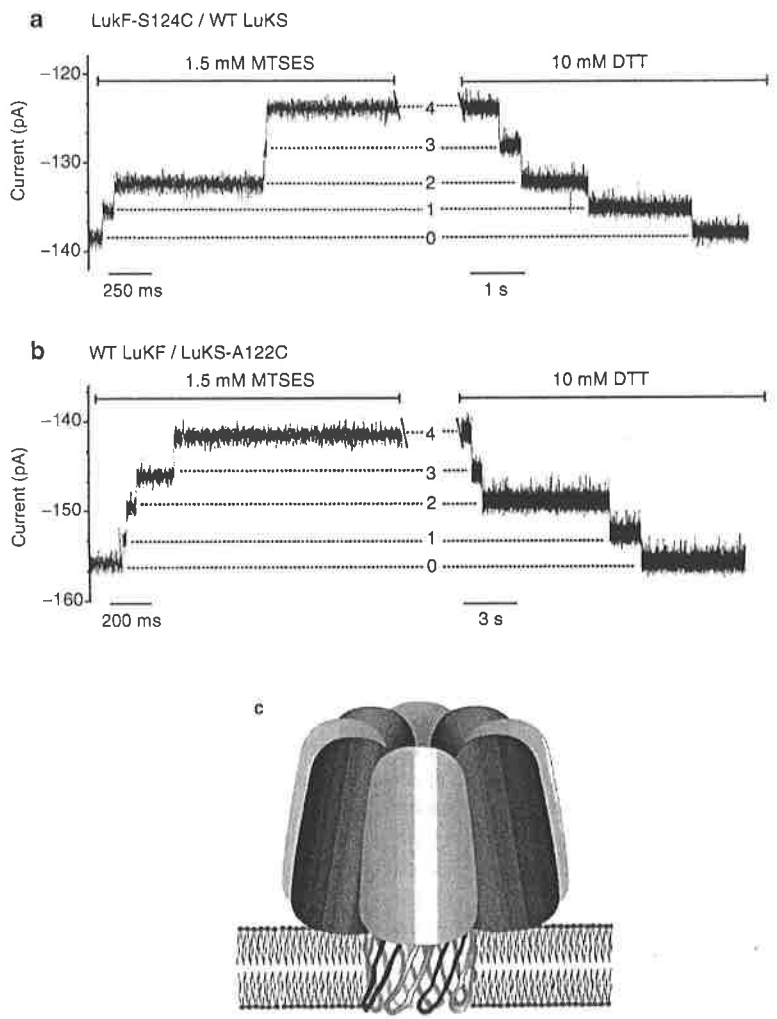

Fig. 10.6 Subunit stoichiometry of a bi-component leukocidin (LukF/LukS) protein complex can be determined using single-channel electrical recordings, membrane protein design, and chemical modification. (**a**) Single-channel electrical recordings probing cysteine Luk mutant LukF-S124C/WT LukS reacted with MTSES; (**b**) Single-channel electrical recordings probing cysteine Luk mutant WT LukF/LukS A122C reacted with MTSES. Here, WT stands for wild type. Permanent cleavage of MTSES from the protein surface was achieved after direct application of the DTT reducing agent to the chamber. The number of reacted individual cysteine sulfhydryls is displayed on the central part of each panel, in between the traces; (**c**) A simplified cartoon of the model of the staphylococcal LukF/LukS pore complex. Each type of polypeptide contributes four subunits to the entire octameric protein complex. LukF is marked in dark grey, whereas LukS is marked in light grey. This model suggests that the leukocidin channel is a 16-stranded β-barrel with an alternating distribution of LukF and LukS, featuring a four-fold symmetry (Table 10.1). In (**a**, **b**), the buffer solution contained 1 M KCl, 50 mM Tris.HCl, 200 μM DTT, 100 μM EDTA, pH 8. The applied transmembrane potential was −60 mV. The single-channel electrical traces were low-pass Bessel filtered at 0.5 kHz (Reproduced, with permission, from Reference (Miles et al. 2002b))

units (Sugawara-Tomita et al. 2002). Such parallel studies from two different groups, offering two distinct outcomes to the same question, have ignited controversies over the true subunit composition of the staphylococcal bi-component β-PFTs. This was especially true, given the lack of the availability of the high-resolution X-ray crystal structure of any leukotoxin complex. Further work by Jayasinghe and Bayley, using chemical cross-linking and clever protein engineering, has confirmed that the LukF/LukS complex is indeed an octamer formed by four LukF and four LukS subunits (Jayasinghe and Bayley 2005). Moreover, using the fusion of LukF with LukS, they showed that the Luk oligomer features a four-fold symmetry with alternating LukF and LukS subunits.

More recently, Tanaka and Kamio's groups have been able to crystalize γHL protein complex at 2.5 Å resolution (Yamashita et al. 2011). This was indeed a breakthrough in the field of staphylococcal β-PFTs, because it was the first crystal structure of a bi-component β-PFT, and it was the first structure of a heteromeric transmembrane β-barrel protein complex. Remarkably, the structure of the complex revealed an octamer with a four-fold symmetry axis about which LukF and Hlg2 alternate. This discovery is consistent with the previous biophysical and biochemical examinations in Bayley's group (Miles et al. 2002b; Jayasinghe and Bayley 2005) and contrasts with early high-resolution electron microscopy and chemical cross-linking experiments using γHL (Sugawara-Tomita et al. 2002). The structure of γHL features a mushroom shape, closely similar with αHL, with the largest diameter of the cap measuring 114 Å, whereas the length of the pore lumen is 93 Å. Interestingly, the internal diameter of the cylindrical β-barrel domain, excluding the side chains of the internal residues is ~25.5 Å, again similar to that of αHL (~26 Å), whereas its total length is ~47 Å. It is surprising that despite its additional subunit, as compared to αHL, the internal dimensions as well as the overall internal shape of the lumen resemble those of αHL. This finding is in accord with a much smaller difference between the unitary conductance of γHL (~115 pS, HlgA/HlgB) and αHL (~92 pS) recorded in 100 mM NaCl (Table 10.2) (Menestrina 1986; Comai et al. 2002). Moreover, a smaller conductance of αHL might be explained by the presence of very bulky residues (e.g., Met-113, Lys-147) forming the central constriction of the pore lumen (Song et al. 1996). Each γHL protomer is made by three domains: cap, rim and stem.

Given this structural information on the staphylococcal bi-component γHL octamer, Yamashita and colleagues have proposed a schematic model for its momomer binding, dimerization, pre-pore formation, and pore assembly (Yamashita et al. 2011) (Fig. 10.7). The monomer binding to the surface is mediated by LukF via a cluster of hydrophobic residues. This hydrophobic cluster includes Tyr72, Trp257, Phe260, and Tyr261 (marked in red). Other residues that are marked in green, including Arg-198, form hydrophilic interface contacts with the headgroups of the bilayer lipids, just in the proximity of the membrane surface. Interface 1, which is exposed upon LukF binding to the membrane, mediates the contact interactions for the dimerization process of LukF-Hlg2. The dimerization undergoes a reorientation process, which activates the dimer for its participation in the pre-pore formation. This process is followed by the pre-stem unfolding from the cap domain,

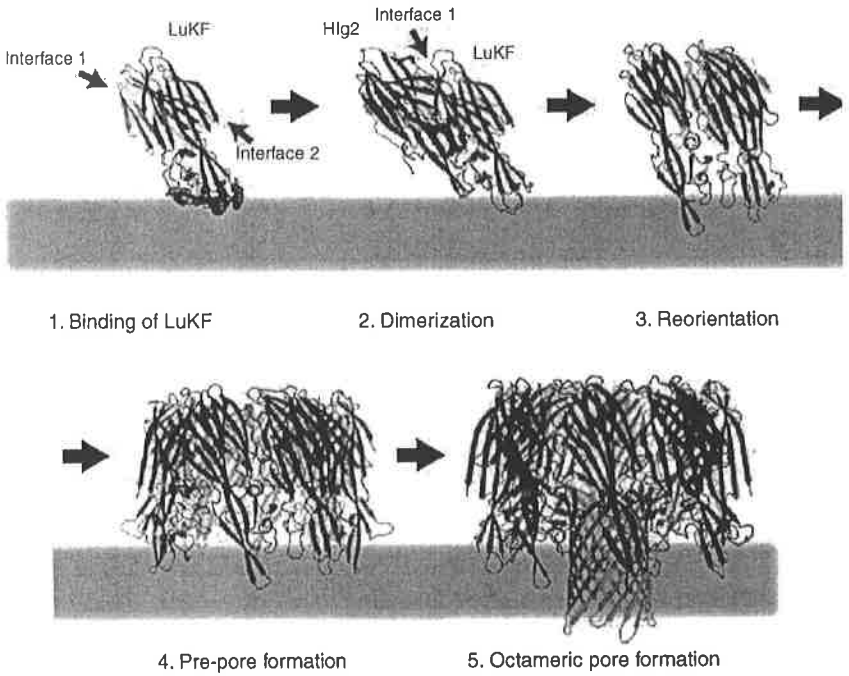

Fig. 10.7 A step-wise model of the oligomerization and assembly of γHL. This model reveals that the initiation process is governed by the spontaneous binding (1) of LukF to the surface of the lipid bilayer, which is illustrated by a gray horizontal bar. The binding of LukF to the membrane surface occurs via a hydrophobic cluster of residues, which includes Tyr72, Trp257, Phe260, and Tyr261 (indicated in *red*). This process is also mediated by Trp177 and Arg198 (marked by *green spheres*). This initial step is followed by a dimerization process (2) of the LukF-Hlg2 complex. Then, the heterodimer undergoes a re-orientation transformation (3) to bring about the dimer from an inactivated to an activated state. Such a transition enables a rapid heteromer growth into tetramers, hexamers, and ultimately octamers, generating the pre-pore formation (4). This process will lead to the complete assembly of the octameric γHL transmembrane pore (5), featuring a four-fold symmetry (Reproduced, with permission, from Reference (Yamashita et al. 2011). Copyright © (2011) National Academy of Sciences, U.S.A.)

triggering its full partitioning into the hydrophobic side of the bilayer as a bi-component transmembrane β-barrel pore.

10.7 Conclusions

This chapter represents a very brief overview of the extensive developments on the structure and function of staphylococcal β-PFTs. The αHL protein is indeed the archetype of the β-PFTs. There are many commonalities of these transmembrane β-barrel proteins. They form mushroom-shaped pore structures on lipid bilayers of

model and cell membranes. The cap domain serves at least two tasks: (i) a large hydrophilic part of the polypeptide makes it water soluble during its navigation from the secreting to attacked cell, and (ii) a large geometrical obstruction would control the partitioning of the β-barrel part into the bilayer and would anchor the protein into the lipid membrane via its rim domain. This particular structure is attained after complex structural transformations of the monomer, in the case of the homomeric toxin, or the dimer, in the case of the bi-component β-PFTs. The transition of water-soluble monomeric form to the transmembrane pore shows the richness and versatility of the protein scaffold for unusual adaptations from the aqueous phase to hydrophobic milieu of the lipid bilayer. The diversity of staphylococcal bi-component β-PFTs has evolutionary been accomplished by pivotal mutations at the protomer-protomer and monomer-membrane interfaces. Staphylococcal β-PFTs are weakly selective with a preference for anions and cations for homomeric and bi-component toxins, respectively. The latter is mainly determined by the presence of an electrostatic selectivity filter, which consists of a cluster of negatively charged residues, on the pore opening near the cap domain. Recent functional and crystallographic studies represent a solid platform for further protein engineering developments of these β-PFTs with great prospects in numerous areas of fundamental and clinical biomedical nanotechnology.

Acknowledgments We are grateful to members of the Movileanu laboratory for their constructive comments. We realized the challenging nature of writing a chapter about a β-barrel toxin that has transformed the area of nanopore biophysics. Therefore, we regret that due to space limitations we were unable to introduce all exciting publications pertinent to this field. This work was supported by the National Institutes of Health, Grant GM088403 (to L.M.).

References

Akeson M, Branton D, Kasianowicz JJ, Brandin E, Deamer DW (1999) Microsecond time-scale discrimination among polycytidylic acid, polyadenylic acid, and polyuridylic acid as homopolymers or as segments within single RNA molecules. Biophys J 77:3227–3233

Aksimentiev A, Schulten K (2005) Imaging {alpha}-Hemolysin with Molecular Dynamics: Ionic Conductance, Osmotic Permeability, and the Electrostatic Potential Map. Biophys J 88:3745–3761

Alonzo F III, Torres VJ (2014) The bicomponent pore-forming leucocidins of Staphylococcus aureus. Microbiol Mol Biol Rev 78:199–230

Astier Y, Bayley H, Howorka S (2005) Protein components for nanodevices. Curr Opin Chem Biol 9:576–584

Baaken G, Ankri N, Schuler AK, Ruhe J, Behrends JC (2011) Nanopore-based single-molecule mass spectrometry on a lipid membrane microarray. ACS Nano 5:8080–8088

Balijepalli A, Ettedgui J, Cornio AT, Robertson JW, Cheung KP, Kasianowicz JJ, Vaz C (2014) Quantifying short-lived events in multistate ionic current measurements. ACS Nano 8:1547–1553

Bayley H (2006) Sequencing single molecules of DNA. Curr Opin Chem Biol 10:628–637

Bayley H, Braha O, Cheley S, Gu LQ (2004) Engineered nanopores. In: Mirkin CA, Niemeyer CM (eds) NanoBiotechnology. Wiley-VCH Verlag GmbH & Co. KGaA, Weinheim, pp 93–112

Bayley H, Cremer PS (2001) Stochastic sensors inspired by biology. Nature 413:226–230

Bayley H, Jayasinghe L (2004) Functional engineered channels and pores (review). Mol Membr Biol 21:209–220
Benner S, Chen RJ, Wilson NA, Abu-Shumays R, Hurt N, Lieberman KR, Deamer DW, Dunbar WB, Akeson M (2007) Sequence-specific detection of individual DNA polymerase complexes in real time using a nanopore. Nat Nanotechnol 2:718–724
Bezrukov SM (2000) Ion channels as molecular Coulter counters to probe metabolite transport. J Membr Biol 174:1–13
Bezrukov SM, Kasianowicz JJ (1993) Current noise reveals protonation kinetics and number of ionizable sites in an open protein ion channel. Phys Rev Lett 70:2352–2355
Bezrukov SM, Krasilnikov OV, Yuldasheva LN, Berezhkovskii AM, Rodrigues CG (2004) Field-Dependent Effect of Crown Ether (18-Crown-6) on Ionic Conductance of {alpha}-Hemolysin Channels. Biophys J 87:3162–3171
Bezrukov SM, Vodyanoy I, Brutyan RA, Kasianowicz JJ (1996) Dynamics and free energy of polymers partitioning into a nanoscale pore. Macromolecules 29:8517–8522
Bischofberger M, Gonzalez MR, van der Goot FG (2009) Membrane injury by pore-forming proteins. Curr Opin Cell Biol 21:589–595
Braha O, Walker B, Cheley S, Kasianowicz JJ, Song LZ, Gouaux JE, Bayley H (1997) Designed protein pores as components for biosensors. Chem Biol 4:497–505
Branton D, Deamer DW, Marziali A, Bayley H, Benner SA, Butler T, Di Ventra M, Garaj S, Hibbs A, Huang X, Jovanovich SB, Krstic PS, Lindsay S, Ling XS, Mastrangelo CH, Meller A, Oliver JS, Pershin YV, Ramsey JM, Riehn R, Soni GV, Tabard-Cossa V, Wanunu M, Wiggin M, Schloss JA (2008) The potential and challenges of nanopore sequencing. Nat Biotechnol 26:1146–1153
Brochard-Wyart F, De Gennes P-G, Sandre O (2000) Transient pores in stretched vesicles: role of leak-out. Physica A 278:32–51
Cheley S, Malghani MS, Song LZ, Hobaugh M, Gouaux JE, Yang J, Bayley H (1997) Spontaneous oligomerization of a staphylococcal alpha-hemolysin conformationally constrained by removal of residues that form the transmembrane beta-barrel. Protein Eng 10:1433–1443
Cherf GM, Lieberman KR, Rashid H, Lam CE, Karplus K, Akeson M (2012) Automated forward and reverse ratcheting of DNA in a nanopore at 5-A precision. Nat Biotechnol 30:344–348
Comai M, Serra MD, Coraiola M, Werner S, Colin DA, Monteil H, Prevost G, Menestrina G (2002) Protein engineering modulates the transport properties and ion selectivity of the pores formed by staphylococcal gamma- haemolysins in lipid membranes. Molecular Microbiology 44:1251–1267
Czajkowsky DM, Sheng ST, Shao ZF (1998) Staphylococcal alpha-hemolysin can form hexamers in phospholipid bilayers. J Mol Biol 276:325–330
De Gennes P-G (1999a) Flexible polymers in nanopores. Adv Polym Sci 138:91–105
De Gennes P-G (1999b) Passive entry of a DNA molecule into a small pore. Proc Natl Acad Sci U S A 96:7262–7264
De Gennes P-G (1999c) Problems of DNA entry into a cell. Physica A 274:1–7
DuMont AL, Torres VJ (2014) Cell targeting by the Staphylococcus aureus pore-forming toxins: it's not just about lipids. Trends Microbiol 22:21–27
Fang Y, Cheley S, Bayley H, Yang J (1997) The heptameric prepore of a Staphylococcal alpha-hemolysin mutant in lipid bilayers imaged by atomic force microscopy. Biochemistry 36:9518–9522
Ferreras M, Hoper F, Dalla Serra M, Colin DA, Prevost G, Menestrina G (1998) The interaction of Staphylococcus aureus bi-component gamma- hemolysins and leucocidins with cells and lipid membranes. Biochim Biophys Acta -Biomembr 1414:108–126
Gonzalez MR, Bischofberger M, Pernot L, van der Goot FG, Freche B (2008) Bacterial pore-forming toxins: the (w)hole story? Cell Mol Life Sci 65:493–507
Goodrich CP, Kirmizialtin S, Huyghues-Despointes BM, Zhu AP, Scholtz JM, Makarov DE, Movileanu L (2007) Single-molecule electrophoresis of beta-hairpin peptides by electrical recordings and Langevin dynamics simulations. J Phys Chem B 111:3332–3335

Gouaux E (1998) Alpha-hemolysin from staphylococcus aureus: an archetype of beta-barrel, channel-forming toxins. J Struct Biol 121:110–122
Gouaux E, Hobaugh M, Song LZ (1997) Alpha-hemolysin, gamma-hemolysin, and leukocidin from staphylococcus aureus: distant in sequence but similar in structure. Protein Sci 6:2631–2635
Gouaux JE, Braha O, Hobaugh MR, Song LZ, Cheley S, Shustak C, Bayley H (1994) Subunit stoichiometry of staphylococcal Alfa-hemolysin in crystals and on membranes - a heptameric transmembrane pore. Proc Natl Acad Sci U S A 91:12828–12831
Gu LQ, Bayley H (2000) Interaction of the noncovalent molecular adapter, beta- cyclodextrin, with the staphylococcal alpha-hemolysin pore. Biophys J 79:1967–1975
Gu LQ, Braha O, Conlan S, Cheley S, Bayley H (1999) Stochastic sensing of organic analytes by a pore-forming protein containing a molecular adapter. Nature 398:686–690
Gu LQ, Cheley S, Bayley H (2003) Electroosmotic enhancement of the binding of a neutral molecule to a transmembrane pore. Proc Natl Acad Sci U S A 100:15498–15503
Guillet V, Roblin P, Werner S, Coraiola M, Menestrina G, Monteil H, Prevost G, Mourey L (2004) Crystal structure of leucotoxin S component: new insight into the Staphylococcal beta-barrel pore-forming toxins. J Biol Chem 279:41028–41037
Gurnev PA, Nestorovich EM (2014) Channel-forming bacterial toxins in biosensing and macromolecule delivery. Toxins (Basel) 6:2483–2540
Hall AR, Scott A, Rotem D, Mehta KK, Bayley H, Dekker C (2010) Hybrid pore formation by directed insertion of alpha-haemolysin into solid-state nanopores. Nat Nanotechnol 5:874–877
Heuck AP, Tweten RK, Johnson AE (2001) Beta-Barrel pore-forming toxins: intriguing dimorphic proteins. Biochemistry 40:9065–9073
Holden MA, Jayasinghe L, Daltrop O, Mason A, Bayley H (2006) Direct transfer of membrane proteins from bacteria to planar bilayers for rapid screening by single-channel recording. Nat Chem Biol 2:314–318
Hornblower B, Coombs A, Whitaker RD, Kolomeisky A, Picone SJ, Meller A, Akeson M (2007) Single-molecule analysis of DNA-protein complexes using nanopores. Nat Methods 4:315–317
Howorka S, Movileanu L, Lu XF, Magnon M, Cheley S, Braha O, Bayley H (2000) A protein pore with a single polymer chain tethered within the lumen. J Am Chem Soc 122:2411–2416
Howorka S, Siwy Z (2008) Nanopores: generation, engineering and single-molecule applications. In: Hinterdorfer P (ed) Handbook of single-molecule biophysics. Springer, New York
Howorka S, Siwy Z (2009) Nanopore analytics: sensing of single molecules. Chem Soc Rev 38:2360–2384
Iacovache I, Bischofberger M, van der Goot FG (2010) Structure and assembly of pore-forming proteins. Curr Opin Struct Biol 20:241–246
Iacovache I, van der Goot FG, Pernot L (2008) Pore formation: an ancient yet complex form of attack. Biochim Biophys Acta 1778:1611–1623
Jayasinghe L, Bayley H (2005) The leukocidin pore: evidence for an octamer with four LukF subunits and four LukS subunits alternating around a central axis. Protein Sci 14:2550–2561
Jung Y, Bayley H, Movileanu L (2006) Temperature-responsive protein pores. J Am Chem Soc 128:15332–15340
Kang XF, Gu LQ, Cheley S, Bayley H (2005) Single protein pores containing molecular adapters at high temperatures. Angew Chem Int Ed Engl 44:1495–1499
Kasianowicz JJ, Bezrukov SM (1995) Protonation dynamics of the alpha-toxin ion-channel from spectral-analysis of ph-dependent current fluctuations. Biophys J 69:94–105
Kasianowicz JJ, Brandin E, Branton D, Deamer DW (1996) Characterization of individual polynucleotide molecules using a membrane channel. Proc Natl Acad Sci U S A 93:13770–13773
Kolomeisky AB (2007) Channel-facilitated molecular transport across membranes: attraction, repulsion, and asymmetry. Phys Rev Lett 98:048105
Kolomeisky AB (2008) How polymers translocate through pores: memory is important. Biophys J 94:1547–1548

Kong CY, Muthukumar M (2005) Simulations of stochastic sensing of proteins. J Am Chem Soc 127:18252–18261
Korchev YE, Alder GM, Bakhramov A, Bashford CL, Joomun BS, Sviderskaya EV, Usherwood PN, Pasternak CA (1995) Staphylococcus aureus alpha-toxin-induced pores: channel-like behavior in lipid bilayers and patch clamped cells. J Membr Biol 143:143–151
Krasilnikov OV, Bezrukov SM (2004) Polymer partitioning from nonideal solutions into protein voids. Macromolecules 37:2650–2657
Krasilnikov OV, Merzlyak PG, Yuldasheva LN, Rodrigues CG, Bhakdi S, Valeva A (2000) Electrophysiological evidence for heptameric stoichiometry of ion channels formed by Staphylococcus aureus alpha-toxin in planar lipid bilayers. Molecular Microbiology 37:1372–1378
Krasilnikov OV, Rodrigues CG, Bezrukov SM (2006) Single polymer molecules in a protein nanopore in the limit of a strong polymer-pore attraction. Phys Rev Lett 97:018301
Kusters I, van Oijen AM, Driessen AJ (2014) Membrane-on-a-chip: microstructured silicon/silicon-dioxide chips for high-throughput screening of membrane transport and viral membrane fusion. ACS Nano 8:3380–3392
Los FC, Randis TM, Aroian RV, Ratner AJ (2013) Role of pore-forming toxins in bacterial infectious diseases. Microbiol Mol Biol Rev 77:173–207
Maffeo C, Bhattacharya S, Yoo J, Wells D, Aksimentiev A (2012) Modeling and simulation of ion channels. Chem Rev 112:6250–6284
Maglia G, Heron AJ, Hwang WL, Holden MA, Mikhailova E, Li Q, Cheley S, Bayley H (2009) Droplet networks with incorporated protein diodes show collective properties. Nat Nanotechnol 4:437–440
Maglia G, Restrepo MR, Mikhailova E, Bayley H (2008) Enhanced translocation of single DNA molecules through {alpha}-hemolysin nanopores by manipulation of internal charge. Proc Natl Acad Sci U S A 105:19720–19725
Majd S, Yusko EC, Billeh YN, Macrae MX, Yang J, Mayer M (2010) Applications of biological pores in nanomedicine, sensing, and nanoelectronics. Curr Opin Biotechnol 21:439–476
Mayer M, Yang J (2013) Engineered ion channels as emerging tools for chemical biology. Acc Chem Res 46:2998–3008
Meller A, Nivon L, Brandin E, Golovchenko J, Branton D (2000) Rapid nanopore discrimination between single polynucleotide molecules. Proc Natl Acad Sci U S A 97:1079–1084
Menestrina G (1986) Ionic channels formed by staphylococcus-aureus alpha-toxin – voltage-dependent inhibition by divalent and trivalent cations. J Membr Biol 90:177–190
Menestrina G, Dalla Serra M, Prevost G (2001) Mode of action of beta-barrel pore-forming toxins of the staphylococcal alpha-hemolysin family. Toxicon 39:1661–1672
Menestrina G, Dalla SM, Comai M, Coraiola M, Viero G, Werner S, Colin DA, Monteil H, Prevost G (2003) Ion channels and bacterial infection: the case of beta-barrel pore-forming protein toxins of Staphylococcus aureus. FEBS Lett 552:54–60
Miles G, Bayley H, Cheley S (2002a) Properties of Bacillus cereus hemolysin II: a heptameric transmembrane pore. Protein Sci 11:1813–1824
Miles G, Cheley S, Braha O, Bayley H (2001) The staphylococcal leukocidin bicomponent toxin forms large ionic channels. Biochemistry 40:8514–8522
Miles G, Movileanu L, Bayley H (2002b) Subunit composition of a bicomponent toxin: staphylococcal leukocidin forms an octameric transmembrane pore. Protein Sci 11:894–902
Misakian M, Kasianowicz JJ (2003) Electrostatic influence on ion transport through the alphaHL channel. J Membr Biol 195:137–146
Mohammad MM, Iyer R, Howard KR, McPike MP, Borer PN, Movileanu L (2012) Engineering a rigid protein tunnel for biomolecular detection. J Am Chem Soc 134:9521–9531
Mohammad MM, Movileanu L (2010) Impact of distant charge reversals within a robust beta-barrel protein pore. J Phys Chem B 114:8750–8759
Montoya M, Gouaux E (2003) Beta-barrel membrane protein folding and structure viewed through the lens of alpha-hemolysin. Biochim Biophys Acta 1609:19–27

Movileanu L (2008) Squeezing a single polypeptide through a nanopore. Soft Matter 4:925–931
Movileanu L (2009) Interrogating single proteins through nanopores: challenges and opportunities. Trends Biotechnol 27:333–341
Movileanu L, Bayley H (2001) Partitioning of a polymer into a nanoscopic protein pore obeys a simple scaling law. Proc Natl Acad Sci U S A 98:10137–10141
Movileanu L, Cheley S, Bayley H (2003) Partitioning of individual flexible polymers into a nanoscopic protein pore. Biophys J 85:897–910
Movileanu L, Cheley S, Howorka S, Braha O, Bayley H (2001) Location of a constriction in the lumen of a transmembrane pore by targeted covalent attachment of polymer molecules. J Gen Physiol 117:239–251
Movileanu L, Howorka S, Braha O, Bayley H (2000) Detecting protein analytes that modulate transmembrane movement of a polymer chain within a single protein pore. Nat Biotechnol 18:1091–1095
Movileanu L, Schmittschmitt JP, Scholtz JM, Bayley H (2005) Interactions of the peptides with a protein pore. Biophys J 89:1030–1045
Muthukumar M (1999) Polymer translocation through a hole. J Chem Phys 111:10371–10374
Muthukumar M (2007) Mechanism of DNA transport through pores. Annu Rev Biophys Biomol Struct 36:435–450
Nivala J, Marks DB, Akeson M (2013) Unfoldase-mediated protein translocation through an alpha-hemolysin nanopore. Nat Biotechnol 31:247–250
Noskov SY, Im W, Roux B (2004) Ion permeation through the alpha-hemolysin channel: theoretical studies based on Brownian dynamics and Poisson-Nernst-Plank electrodiffusion theory. Biophys J 87:2299–2309
Olson R, Nariya H, Yokota K, Kamio Y, Gouaux E (1999) Crystal structure of Staphylococcal LukF delineates conformational changes accompanying formation of a transmembrane channel. Nat Struct Biol 6:134–140
Otto M (2014) Staphylococcus aureus toxins. Curr Opin Microbiol 17:32–37
Parker MW, Feil SC (2005) Pore-forming protein toxins: from structure to function. Prog Biophys Mol Biol 88:91–142
Pedelacq JD, Maveyraud L, Prevost G, Baba-Moussa L, Gonzalez A, Courcelle E, Shepard W, Monteil H, Samama JP, Mourey L (1999) The structure of a Staphylococcus aureus leucocidin component (LukF-PV) reveals the fold of the water-soluble species of a family of transmembrane pore-forming toxins. Structure 7:277–287
Potrich C, Bastiani H, Colin DA, Huck S, Prevost G, Dalla SM (2009) The influence of membrane lipids in Staphylococcus aureus gamma-hemolysins pore formation. J Membr Biol 227:13–24
Prevost G, Mourey L, Colin DA, Menestrina G (2001) Staphylococcal pore-forming toxins. Pore-Forming Toxins 257:53–83
Reiner JE, Kasianowicz JJ, Nablo BJ, Robertson JW (2010) Theory for polymer analysis using nanopore-based single-molecule mass spectrometry. Proc Natl Acad Sci U S A 107:12080–12085
Robertson JW, Kasianowicz JJ, Reiner JE (2010) Changes in ion channel geometry resolved to sub-angstrom precision via single molecule mass spectrometry. J Phys Condens Matter 22:454108
Robertson JW, Rodrigues CG, Stanford VM, Rubinson KA, Krasilnikov OV, Kasianowicz JJ (2007) Single-molecule mass spectrometry in solution using a solitary nanopore. Proc Natl Acad Sci U S A 104:8207–8211
Rodrigues CG, Machado DC, Chevtchenko SF, Krasilnikov OV (2008) Mechanism of KCl enhancement in detection of nonionic polymers by nanopore sensors. Biophys J 95:5186–5192
Rodriguez-Larrea D, Bayley H (2013) Multistep protein unfolding during nanopore translocation. Nat Nanotechnol 8:288–295
Sackmann B, Neher E (1995) Single-channel recording. Kluwer Academic/Plenum Publishers, New York

Sanchez-Quesada J, Ghadiri MR, Bayley H, Braha O (2000) Cyclic peptides as molecular adapters for a pore-forming protein. J Am Chem Soc 122:11757–11766
Siwy ZS, Howorka S (2010) Engineered voltage-responsive nanopores. Chem Soc Rev 39:1115–1132
Slonkina E, Kolomeisky AB (2003) Polymer translocation through a long nanopore. J Chem Phys 118:7112–7118
Song LZ, Hobaugh MR, Shustak C, Cheley S, Bayley H, Gouaux JE (1996) Structure of staphylococcal alpha-hemolysin, a heptameric transmembrane pore. Science 274:1859–1866
Sugawara-Tomita N, Tomita T, Kamio Y (2002) Stochastic assembly of two-component staphylococcal gamma- hemolysin into heteroheptameric transmembrane pores with alternate subunit arrangements in ratios of 3: 4 and 4: 3. J Bacteriol 184:4747–4756
Sutherland TC, Long YT, Stefureac RI, Bediako-Amoa I, Kraatz HB, Lee JS (2005) Structure of peptides investigated by nanopore analysis. Nano Lett 4:1273–1277
Tian P, Andricioaei I (2005) Repetitive pulling catalyzes co-translocational unfolding of barnase during import through a mitochondrial pore. J Mol Biol 350:1017–1034
Walker B, Bayley H (1995) Restoration of pore-forming activity in staphylococcal alfa-hemolysin by targeted covalent modification. Protein Eng 8:491–495
Wang HY, Gu Z, Cao C, Wang J, Long YT (2013a) Analysis of a single alpha-synuclein fibrillation by the Interaction with a Protein Nanopore. Anal Chem 85:8254–8261
Wang S, Haque F, Rychahou PG, Evers BM, Guo P (2013b) Engineered nanopore of Phi29 DNA-packaging motor for real-time detection of single colon cancer specific antibody in serum. ACS Nano 7:9814–9822
Wang Y, Zheng D, Tan Q, Wang MX, Gu LQ (2011) Nanopore-based detection of circulating microRNAs in lung cancer patients. Nat Nanotechnol 6:668–674
Wells DB, Abramkina V, Aksimentiev A (2007) Exploring transmembrane transport through alpha-hemolysin with grid-steered molecular dynamics. J Chem Phys 127:125101
Werner S, Colin DA, Coraiola M, Menestrina G, Monteil H, Prevost G (2002) Retrieving biological activity from LukF-PV mutants combined with different S components implies compatibility between the stem domains of these staphylococcal bicomponent leucotoxins. Infect Immun 70:1310–1318
White SH, Wimley WC (1999) Membrane protein folding and stability: physical principles. Annu Rev Biophys Biomol Struct 28:319–365
Wimley WC (2003) The versatile beta-barrel membrane protein. Curr Opin Struct Biol 13:404–411
Yamashita K, Kawai Y, Tanaka Y, Hirano N, Kaneko J, Tomita N, Ohta M, Kamio Y, Yao M, Tanaka I (2011) Crystal structure of the octameric pore of staphylococcal gamma-hemolysin reveals the beta-barrel pore formation mechanism by two components. Proc Natl Acad Sci U S A 108:17314–17319
Yoong P, Torres VJ (2013) The effects of Staphylococcus aureus leukotoxins on the host: cell lysis and beyond. Curr Opin Microbiol 16:63–69

Chapter 11
Properties of Pores Formed by Cholesterol-Dependent Cytolysins and Actinoporins

Nejc Rojko, Manuela Zanetti, Gregor Anderluh, and Mauro Dalla Serra

Abstract Planar lipid membrane (PLM) measurements allow direct observation of pores in model lipid membranes. This biophysical approach was very important for our understanding of how transmembrane pores are formed by cholesterol-dependent cytolysins (CDCs), a toxin family from pathogenic bacteria, and actinoporins, cytolysins from sea anemones. In this review we discuss current knowledge of pore formation by these two protein families and how the PLM approach revealed mechanisms by which these two unrelated protein families porate membranes. Interestingly, for both toxins, the protein portion constituting the pore walls has an alpha helical configuration in the secreted water soluble form. This structure is maintained for actinoporins in the membrane inserted configuration, while the pore of CDCs necessitates a drastic change in secondary structure, which transforms to beta hairpins in the membrane. Both proteins are able to form toroidal proteo-lipid pores.

Keywords Cholesterol-dependent cytolysins • Actinoporins • Pore • Planar lipid membrane

N. Rojko
Laboratory for Molecular Biology and Nanobiotechnology,
National Institute of Chemistry, Hajdrihova 19, Ljubljana 1000, Slovenia
e-mail: nejc.rojko@ki.si

M. Zanetti • M. Dalla Serra
Laboratory of Biomolecular Sequence and Structure Analysis for Health, Istituto di Biofisica,
Consiglio Nazionale delle Ricerche & Fondazione Bruno Kessler,
via alla Cascata 56/C, Trento 38123, Italy
e-mail: mzanetti@fbk.eu; mauro.dallaserra@cnr.it

G. Anderluh (✉)
Laboratory for Molecular Biology and Nanobiotechnology,
National Institute of Chemistry, Hajdrihova 19, Ljubljana 1000, Slovenia

Department of Biology, Biotechnical Faculty, University of Ljubljana,
Jamnikarjeva 101, Ljubljana 1000, Slovenia
e-mail: gregor.anderluh@ki.si

A.H. Delcour (ed.), *Electrophysiology of Unconventional Channels and Pores*,
Springer Series in Biophysics 18, DOI 10.1007/978-3-319-20149-8_11